Fabrication of 3D electrodes for subretinal photovoltaic stimulation

Davidsen, Rasmus Schmidt; Keller, Stephan Sylvest; Bek, Toke; Hansen, Ole

Publication date:
2017

Document Version
Peer reviewed version

Fabrication of 3D electrodes for subretinal photovoltaic stimulation

Rasmus Schmidt Davidsen*[,a], Stephan Sylvest Keller[a], Toke Bek[b], Ole Hansen[a]

[a]*Department of Micro- and Nanotechnology, Technical University of Denmark (DTU)*
[b]*Department of Ophthalmology, Aarhus University Hospital*
**rasda@nanotech.dtu.dk*

Background
Retinal diseases are the most frequent causes of visual loss in the Western world. Two of the prominent diseases are age-related macular degeneration (AMD) diagnosed in 700.000 persons annually alone in the US, and retinitis pigmentosa (RP) which is diagnosed for 1 out of 4000 live births [1]. The detailed pathophysiology of AMD and RP is unknown, but a central event leading to visual loss in these diseases is the degeneration of retinal photoreceptors. At present, there are no effective treatments of photoreceptor degeneration. A promising potential solution for partial restoration of sight is to implant a solar (photovoltaic) cell that can translate the incoming light into an electrical signal to be transmitted to the secondary neurons in the retina [2-5].

A solar cell is a photodiode, which produces an electrical output directly from incoming light in the relevant wavelength range. By placing an array of electrically separated photodiodes or solar cells at the location of lost photoreceptors and in contact with the overlying retina, stimulation of the secondary neurons will occur when light is incident on the eye. The restoration of vision using photodiodes is limited by 1) the resolution (pixel density) of the solar cell array, 2) the sensitivity of the solar cells to the incident light and 3) the connection of the solar cell to the secondary neurons in the retina.

Palanker *et al.* [6,7] demonstrated the fabrication of a photovoltaic array with pixel sizes down to 70×70 μm^2 and a responsivity of 0.36 A/W. Zrenner *et al.* [8] demonstrated a similar array with 1500 photodiodes, and the study confirmed a satisfactory object recognition and overall meaningful detailed vision in previously blind patients. However, it remains a major challenge to obtain a sufficient light sensitivity and optimal connection of an implantable photovoltaic array to the secondary retinal neurons [6-8]. The latter may be improved by creating 3D structures that enhance the migration of retinal tissue and cells into voids and cavities at the tissue-implant interface. It has been reported [9] that pillars with 10 μm diameter, 40 μm height and 40 μm center-to-center spacing lead to significant migration of both Müller cells and inner nuclear layer cells. Such structures were typically defined in the photosensitive polymer SU-8, but no electrically active 3D electrodes for retinal implants have been reported to date.

Objective
In order to improve contact between stimulating electrodes in subretinal photovoltaic implants and the surrounding tissue, electrically active 3D interfaces must be realized. Enhanced charge transfer between stimulating electrodes and the neural tissue may enable a smaller minimum ‘pixel’ area and thereby higher resolution in the prosthetic vision, which is the final goal. We propose a 1-diode subretinal prosthesis design utilizing 3D electrodes made from pyrolytic carbon. The final device would further rely on via holes between isolated electrodes (pixels) enabling sufficient nutrient flow to the cells and charge transport from each local electrode to a common return electrode on the rear of the device. Investigation and fabrication of such a device is ongoing, but this paper focuses on the fabrication of 3D carbon electrodes.
3D carbon electrodes were obtained by pyrolysis of the negative photoresist SU-8 at temperatures above 900℃ in inert atmosphere. SU-8 is very suitable for fabricating high aspect ratio microstructures with

dimensions suitable for subretinal neural stimulation. Pyrolyzed SU-8 has been reported to be biocompatible and promote adhesion and differentiation of certain cells [10]. Thus, 3D pyrolytic carbon electrodes made from SU-8 seem promising for the application in subretinal prosthesis. However, the electrical and mechanical properties of carbon pillar electrodes on silicon must be investigated. More specifically, the contact resistance between carbon and Si has to be minimized and the high process temperatures should not affect the Si photodiode.

Methods

Carbon electrodes were fabricated with a method similar to that shown earlier [11]. SU-8(2075) was spun to a thickness of 78 µm using a Süss MicroTec-RCD8T spin coater. The polymer was softbaked on a hot plate at 50℃ for 5 hours, exposed to a dose of 210 mJ/cm^2 UV radiation and post exposure baked at 50℃ for 5 hours. The structures were developed in PGMEA for 2x10 minutes, treated with a 500 mJ/cm^2 UV 'flood-exposure' and a second hard bake. The SU-8 structures were pyrolyzed in an ATV-PEO604 furnace at 900℃ for 1 hour (with a 30 minute preheat at 200℃), resulting in carbon micropillars with a height of ~ 40 µm. Figure 1 (bottom) shows SEM images of the resulting 3D carbon electrodes.

Contact resistance patterns were fabricated by 1) defining highly n-doped areas in a p-type double-side polished CZ silicon wafer (4" diameter, 350 µm thick, 0.4 Ω-cm) using phosphorus diffusion at 900℃ for 30 minutes with $POCl_3$ as dopant source in a Tempress tube furnace, 2) etching contact windows in the SiO_2 mask using photolithography and buffered HF and 3) fabricating pyrolytic carbon pads from SU-8 according to the methods described previously. Figure 1 (top) shows optical microscope images of the resulting test structures.

The contact resistance between n^+ Si and pyrolytic carbon electrodes was measured on the 'Kelvin resistor' test structures seen in Figure 1 by forcing current through opposing terminals and recording the voltage on the remaining two terminals. The result is shown in Figure 2. Plotting voltage as a function of current is expected to yield a linear relationship with a slope equal to the Kelvin resistance, R_K, defined as [12]:

$$R_K = \frac{\rho_c}{A} + R_g,$$

where ρ_c is the specific contact resistance, A is the contact area and R_g is a parasitic, geometry-dependent resistance term, which may be neglected if the arm width equals the hole width in the design of the Kelvin resistor, such as shown in Figure 1 (top).

Results

Figure 1 (top) shows optical microscope images of the Kelvin resistor test structures. The sidelength of the contact hole in the center was varied between 15-50 µm, the arm width was kept equal to the contact hole sidelength and SU-8 pads were made sufficiently large (1 mm diameter in this case) such that the size of the pads did not affect the resistance measurement. Figure 1 (bottom) shows SEM-images of the 3D carbon electrodes after pyrolysis. Several 2x2 mm^2 arrays consisting of 50x50 pillars with a center-to-center spacing of 40 µm were produced. Figure 1D shows that structures are cylindrical pillars with 36 µm height and 15 µm diameter, which is acceptable considering the target of 40 µm height and 10 µm diameter. However, as seen in Figure 1D, the pillars are tilted and not upright, which is not ideal. Our hypothesis is that neighboring SU-8 structures were not fully resolved but interconnected after photoresist development, which resulted in tilted pillars after pyrolysis. This should be easily solved by decreasing the pillar diameter or increasing the distance between structures. Since the resulting diameter is larger than the target, future work will include a decreased pillar diameter, aiming for 10 µm after pyrolysis.

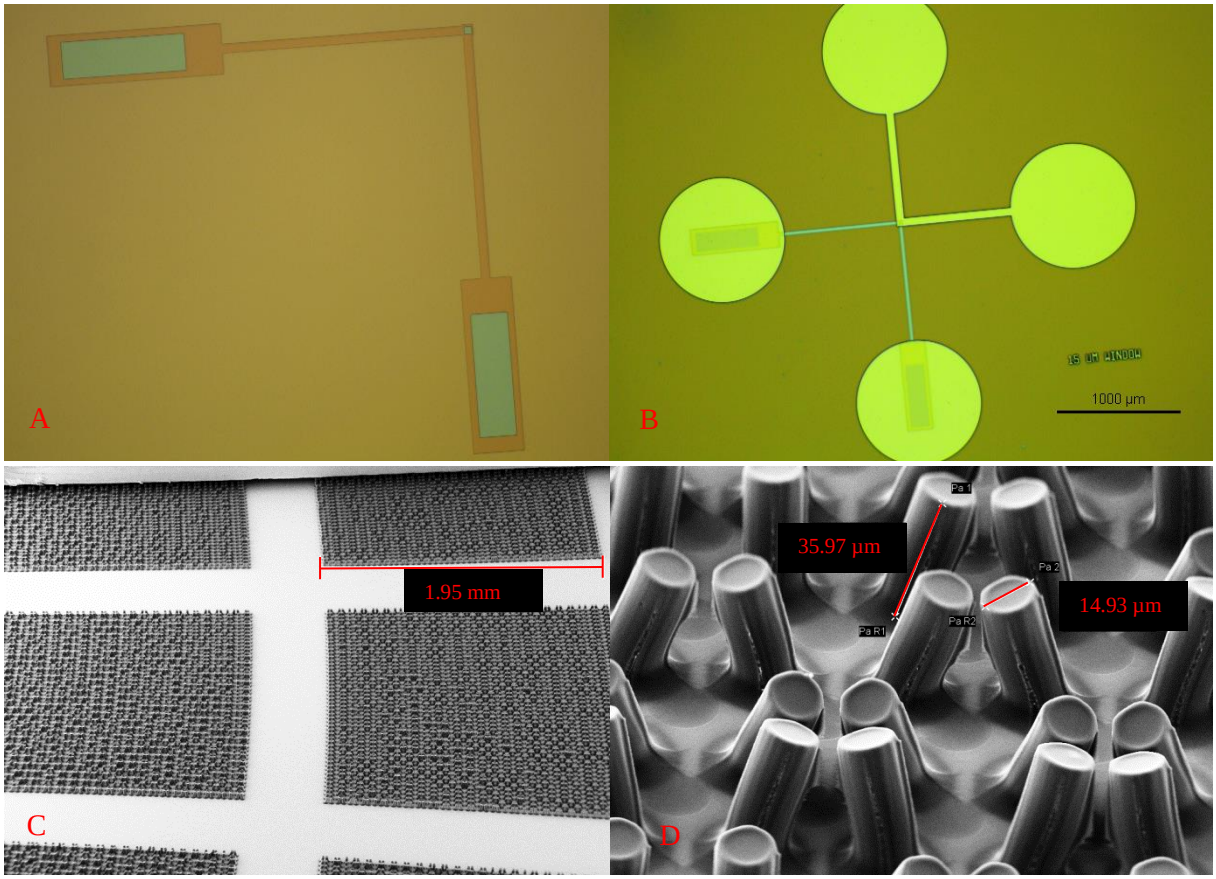

Figure 1: (top) 'Kelvin resistor' test structures with n^+ Si and SiO_2 mask with(A) and without(B) SU8 pads used for contact resistance measurements. ***(bottom)*** SEM-images of carbon electrodes at 72x(C) and 1700x(D) magnification.

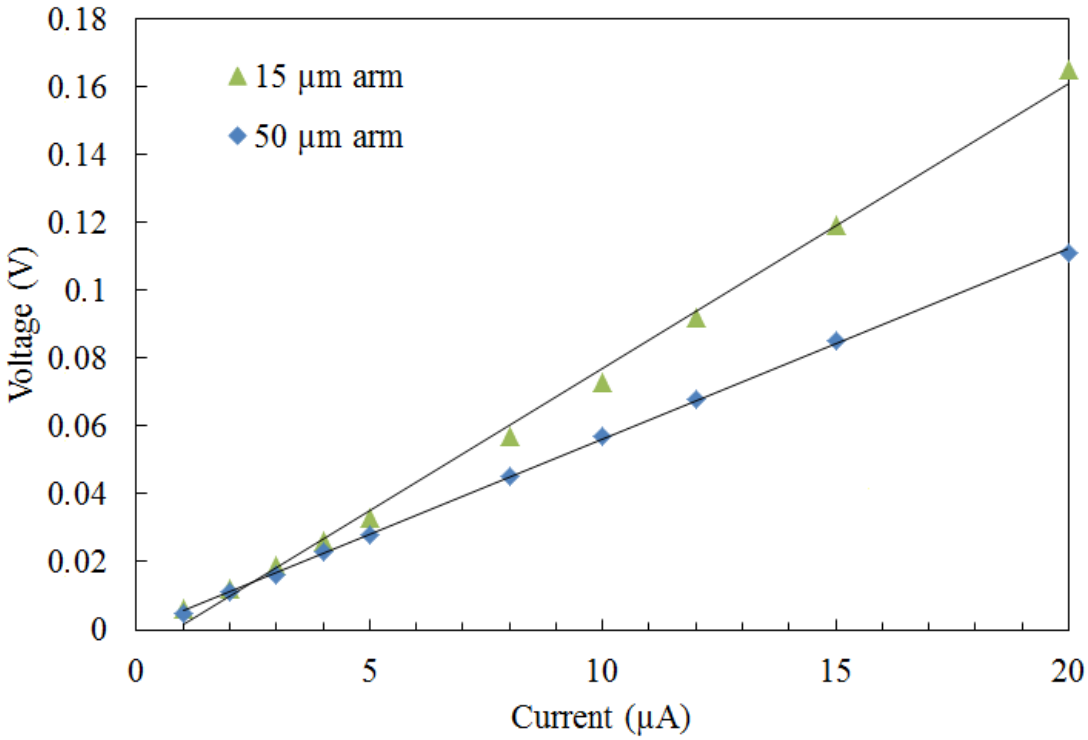

Figure 2: Voltage-current measurement on test structures with pyrolyzed SU-8 contacts on n^+ Si. The linear fit-lines yield slopes of 0.0084 and 0.0056 (Kelvin resistances of 8.4 and 5.6 kΩ) for 15 and 50 µm arm, respectively.

Figure 2 shows the measured voltage at different currents in the range 0-20 µA. The current range was chosen in order to measure in a voltage range significantly lower than the expected operating voltage of ~ 0.6 V for a single-diode silicon photovoltaic device. The linear regressions yield Kelvin resistances of 5.6 and 8.4 kΩ for 50 and 15 µm windows, respectively. This results in specific contact resistances of 140 and 19 mΩcm^2, respectively, simply by multiplying the Kelvin resistance with the contact window area. For a circular contact area with a radius of 7.5 µm, the contact resistance is 33 kΩ, using the value for the 15 µm window, which is more comparable in size with the actual electrode geometry. This may be compared with the spreading resistance, R_{sp}, from a hemispherical electrode with the same radius surrounded by tissue with assumed resistivity of $\rho = 1.67$ Ωm [10,13]:

$$R_{\mathrm{sp}} = \frac{1.67\ \Omega\mathrm{m}}{2\pi \cdot 7.5 \times 10^{-6}\mathrm{m}} = 35\ \mathrm{k}\Omega$$

Thus, since the measured contact resistance is slightly smaller than the spreading resistance, the result confirms that pyrolyzed SU-8 may indeed be used as an electrode material on highly doped Si. However, because the contact resistance is in the same order of magnitude as the spreading resistance, there is still room for improvement in terms of the carbon to silicon contact. This was further indicated by significant delamination of pyrolytic carbon on parts of the wafer observed immediately after pyrolysis.

Furthermore, the sheet resistance of pyrolyzed SU-8 was measured. Van der Pauw structures similar in size and shape to those shown in Figure 1B of SU-8 on top of SiO_2 (i.e. electrically isolated from the underlying Si wafer) were defined and pyrolyzed on the same wafer as the pillar and Kelvin resistor structures described above. After pyrolysis the voltage-current (V-I) relationship was measured on several different van der Pauw structures (two different wafers) and the sheet resistance, R_{sh}, was calculated from the measured resistance, R, extracted as the slope of the linear, ohmic V-I curves, following that [12]

$$R_{\mathrm{sh}} = R \cdot \frac{\pi}{\ln(2)}.$$

Measured resistances were in the range 968-1945 Ω, so the sheet resistance is in the range 4.4-8.8 kΩ. This is significantly higher than expected for pyrolytic carbon [14-15]. Due to the significant delamination of SU8 carbon after pyrolysis the van der Pauw structures were not intact and the uniformity of the layer is therefore rather uncertain. This may have affected the measurement, such that the resistance is dominated by parts of the structure that are thinner or more narrow than intended. However, the measurement may also reveal the actual sheet resistance of the pyrolytic carbon in this case, which means that the SU-8 coating and pyrolysis process should be optimized further. Temperature, time and gas flows during pyrolysis may all affect the resulting sheet resistance significantly [16].
The high sheet resistance may have affected the previously presented contact resistance measurements, such that the actual contact resistance between carbon and Si effectively is lower than what is presented in this work. The sheet resistance of the pyrolytic carbon electrodes needs to be improved significantly in order not to limit charge carrier transport within the carbon electrodes. Preferably, a sheet resistance of ~ 100 Ω should be realized. This should be feasible if the pyrolysis process is optimized. It was observed that the adhesion of the fabricated pillar-structures on Si was much better compared to that on SiO_2 for the van der Pauw structures. Future studies will include fabrication of pyrolyzed SU-8 directly on Si allowing for better adhesion and more accurate determination of the sheet resistance.

Conclusion

The measured contact resistance confirms that pyrolytic carbon is a possible candidate as a 3D electrode material on photovoltaic silicon retinal implants. However, there is still room for improvement on the electrical and mechanical properties of the fabricated structures. In particular, 'tilting' of the pillar electrodes should be avoided and the sheet resistance of the pyrolytic carbon has to be significantly decreased.

Acknowledgements

The authors gratefully acknowledge the funding support from Velux Fonden (project nr. 13891) and Young Investigator Program of the Villum Foundation, project no. VKR023438.

References

[1] J. D. Loudin, D. M. Simanovkskii, K. Vijayraghavan, C. K. Sramek, A. F. Butterwick, P. Huie, G. Y. McLean, D. V. Palanker "Optoelectronic retinal prosthesis: system design and performance" *J. Neural Eng*. **4** (2007) 72-84. doi:10.1088/1741-2560/4/1/S09

[2] Y. Mandel, G. Goetz, D. Lavinsky, P. Huie, K. Mathieson, L. Wang, T. Kamins, L. Galambos, R. Manivanh, J. Harris, D. Palanker "Cortical responses elicited by photovoltaic subretinal prostheses exhibit similarities to visually evoked potentials" *Nature communications* **4** (2013) 1980. doi:10.1038/ncomms2980

[3] S. Y. Kim, S. Sadda, J. Pearlman, M. S. Humayun, E. de Juan Jr, B. M. Melia, W. R. Green "Morphometric analysis of the macula in eyes with disciform age-related macular degeneration" *Retina* **22** (2002) 471–477. doi: 10.1097/00006982-200208000-00012

[4] F. Mazzoni, E. Novelli, E. Strettoi "Retinal ganglioncells survive and maintain normal dendritic morphology in a mouse model of inherited photoreceptor degeneration" *J. Neurosci.* **28** (2008) 14282–14292. doi:10.1523/JNEUROSCI.4968-08.2008

[5] J. L. Stone, W. E. Barlow, M. S. Humayun, E. de Juan Jr, A. H. Milam "Morphometric analysis of macular photoreceptors and ganglion cells in retinas with retinitis pigmentosa" *Arch. Ophthalmol.* **110** (1992) 1634–1639.doi:10.1001/archopht.1992.01080230134038

[6] L. Wang, K. Mathieson, T. I. Kamins, J. D. Loudin, L. Galambos, G. Goetz, J. S. Harris, D. V. Palanker "Photovoltaic retinal prosthesis: implant fabrication and performance" *Journal of Neural Engineering* **9** (2012) 046014. doi:10.1088/1741-2560/9/4/046014

[7] K. Mathieson, J. Loudin, G. Goetz, P. Huie, L. Wang, T. I. Kamins, L. Galambos, R. Smith, J. S. Harris, A. Sher, D. Palanker "Photovoltaic retinal prosthesis with high pixel density" *Nature photonics* **6** (2012) 391-397. doi:10.1038/nphoton.2012.104

[8] E. Zrenner, K. U. Bartz-Schmidt, H. Benav, D. Besch, A. Bruckmann, V. P. Gabel, F. Gekeler, U. Greppmaier, A. Harscher, S. Kibbel, J. Koch, A. Kusnyerik, T. Peters, K. Stingl, H. Sachs, A. Stett, P. Szurman, B. Wilhelm, R. Wilke "Subretinal electronic chips allow blind patients to read letters and combine them to words" *Proceedings of the Royal Society of London B: Biological Sciences* **278** (2011) 1489-1497, doi: 10.1098/rspb.2010.1747

[9] G.A. Goetz, D.V. Palanker, "Electronic approaches to restoration of sight", *Rep. Prog. Phys*. **79** (2016) 096701, doi: 10.1088/0034-4885/79/9/096701

[10] L. Amato, A. Heiskanen, C. Caviglia, F. Shah, K. Zór, M. Skolimowski, M. Madou, L. Gammelgaard, R. Hansen, E.G. Seiz, M. Ramos, T.R. Moreno, A. Martinez-Serrano, S. S. Keller, J. Emnéus, "Pyrolysed 3D-Carbon Scaffolds Induce Spontaneous Differentiation of Human Neural Stem Cells and Facilitate Real-Time Dopamine Detection" *Advanced functional materials*, **24** 44 (2014) 7042-7052, doi: 10.1002/adfm.201400812

[11] S. Hemanth, C. Caviglia, S.S. Keller, "Suspended 3D pyrolytic carbon microelectrodes for electrochemistry", *Carbon* (2017), in press

[12] D.K. Schroder, “Semiconductor material and device characterization”, John Wiley & Sons, (2006).

[13] C. Gabriel, A. Peyman, E.H. Grant, “Electrical conductivity of tissue at frequencies below 1 MHz”, *Phys. Med. Biol.* **54** (2009) 4863–4878, doi: 10.1088/0031-9155/54/16/002

[14] K. Loizos, A.K. RamRakhyani, J. Anderson, R. Marc, G. Lazzi, “On the computation of a retina resistivity profile for applications in multi-scale modeling of electrical stimulation and absorption”, *Phys. Med. Biol.* **61**(12) (2016) 4491–4505, doi: 10.1088/0031-9155/61/12/4491

[15] L. Amato, A. Heiskanen, R. Hansen, L. Gammelgaard, T. Rindzevicius, M. Tenje, J. Emnéus, S.S. Keller, ”Dense high-aspect ratio 3D carbon pillars on interdigitated microelectrode arrays” *Carbon* **94** (2015) 792-803, doi: 10.1016/j.carbon.2015.06.014

[16] Y.M. Hassan, C. Caviglia, S. Hemanth, D.M.A. Mackenzie, T.S. Alstrøm, D.H. Petersen, **S.S.** Keller, “High temperature SU-8 pyrolysis for fabrication of carbon electrodes”, *J. Anal. Appl. Pyrolysis* (2017), In press